Phenotypic Epithelial Changes in Laryngotracheal Stenosis

Ioan A. Lina, MD ; Hsiu-Wen Tsai, PhD ; Alexandra J. Berges, BS ; Rafael A. Ospino, BS ;
Ruth J. Davis, MD ; Kevin M. Motz, MD ; Samuel Collins, PhD; Baishakhi Ghosh, PhD;
Venkataramana Sidhaye, MD; Alexander Gelbard, MD; Alexander T. Hillel, MD

Objective: Characterize and quantify epithelium in multiple etiologies of laryngotracheal stenosis (LTS) to better understand its role in pathogenesis.

Study Design: Controlled in vitro cohort study.

Methods: Endoscopic brush biopsy samples of both normal (non-scar) and scar were obtained in four patients with idiopathic subglottic stenosis (iSGS) and four patients with iatrogenic LTS (iLTS). mRNA expression of basal, ciliary, and secretory cell markers were evaluated using quantitative PCR. Cricotracheal resection tissue samples (n = 5 per group) were also collected, analyzed using quantitative immunohistochemistry, and compared with rapid autopsy tracheal samples.

Results: Both iSGS and iLTS-scar epithelium had reduced epithelial thickness compared with non-scar control epithelium ($P = .0009$ and $P = .0011$, respectively). Basal cell gene and protein expression for cytokeratin 14 was increased in iSGS-scar epithelium compared with iLTS or controls. Immunohistochemical expression of ciliary tubulin alpha 1, but not gene expression, was reduced in both iSGS and iLTS-scar epithelium compared with controls ($P = .0184$ and $P = .0125$, respectively). Both iSGS and iLTS-scar had reductions in Mucin 5AC gene expression ($P = .0007$ and $P = .0035$, respectively), an epithelial goblet cell marker, with reductions in secretory cells histologically ($P < .0001$).

Conclusions: Compared with non-scar epithelium, the epithelium within iSGS and iLTS is morphologically abnormal. Although both iSGS and iLTS have reduced epithelial thickness, ciliary cells, and secretory cells, only iSGS had significant increases in pathological basal cell expression. These data suggest that the epithelium in iSGS and iLTS play a common role in the pathogenesis of fibrosis in these two etiologies of laryngotracheal stenosis.

Setting: Tertiary referral center (2017–2020).

Key Words: Laryngotracheal stenosis, iatrogenic, idiopathic subglottic stenosis, iSGS, iLTS, subglottic stenosis, epithelium.

Level of Evidence: NA

Laryngoscope, 132:2194–2201, 2022

INTRODUCTION

Laryngotracheal stenosis (LTS) is a severe recurrent airway disease that results from scaring of the subglottis, glottis, and/or trachea. Although there are several etiologies of LTS, intubation-related injury (iatrogenic LTS, iLTS) and idiopathic disease (idiopathic subglottic stenosis [iSGS]) are the most predominant.[1] Although there are established clinical differences in patient demographics, disease severity, and prognosis between these two etiologies,[2] iLTS and iSGS both manifest in a common clinical phenotype of obstructive fibrosis limiting physiologic airflow.[1,3] In both cases, patients develop worsening subjective dyspnea secondary to luminal compromise and require procedural intervention to improve ventilation.

The surgical treatment of all types of LTS includes three key principles: excision and/or dilation of scar tissue; restoration of luminal patency; and reconstitution of the innate epithelial barrier. Although open reconstructive treatments such as cricotracheal resection remove disease airway epithelium *en bloc* with the underlying submucosa scar and cartilage framework, newer endoscopic techniques aimed at isolated mucosa resection and epithelial reconstitution have also been explored. Specifically, the Maddern procedure, which involves endoscopic scar excision and barrier replacement with autologous

epithelial substitute (either split-thickness-skin-graft or buccal mucosal grafts), has demonstrated efficacy in reducing scar recurrence.[4,5] These surgical approaches contrast with the mainstay surgical treatment, namely endoscopic excision and balloon dilation, which fails to reconstitute the epithelium and may contribute to scar recurrence and the need for serial procedures.[6] The restoration of airway epithelium as a critical component to durable treatment response for LTS suggests that epithelial defects may play a role in the development, maintenance, or progression of airway fibrosis.[7]

The ciliated pseudostratified columnar epithelium of the subglottis and trachea constitutes a mechanical barrier against pathogens and noxious pollutants, and generates glycoproteins/mucus to neutralize antigens and to facilitate their clearance.[8] These complex functions require a number of specialized cell types including basal cells, secretory cells (goblet or mucus-producing cells and club cells), and ciliated cells for normal, healthy epithelial function (Fig. 1).[9] Recent findings in alternate pulmonary pathologies have placed central importance on airway epithelial barrier function in the pathogenesis of chronic airway disease. For example, ciliary dysfunction contributes to the pathophysiology of primarily ciliary dyskinesia (PCD),[10] as well as chronic obstructive pulmonary disease (COPD), by reducing mucociliary clearance.[11–13] Alternatively, in idiopathic pulmonary fibrosis (IPF), epithelial apoptosis with disruption of the basement membrane secondary to chronic inflammation is a hallmark histologic characteristic. In animal models of IPF, genetic defects in the epithelial barrier are associated with accelerated fibrosis, driven by pathologic lung fibroblasts.[14,15]

The durable clinical outcomes of LTS treatments that restore the epithelial barrier, as well as the involvement of dysfunctional cilia in PCD, COPD, and IPF, suggests that dysfunctional airway epithelial cell types may be a component of LTS pathogenesis. In this study, we sought to characterize the epithelial morphology of two major LTS etiologies (iSGS and iLTS). We hypothesized that LTS airway epithelial morphology is phenotypically different than normal, non-scar epithelium. Further, we hypothesized that patients who develop their injury following prolonged endotracheal intubation would have less ciliated cells than iSGS patients. Our results enhance our understanding of epithelium in LTS scar, provide insight into LTS disease pathogenesis, and may promote innovative new therapies.

METHODS

Epithelial Brush Biopsies and Tissue Section Samples

Endoscopic brush biopsy samples were taken from eight patients, four with iLTS and four with iSGS following informed consent in accordance with the Johns Hopkins University Institutional Review Board (NA_00078310), which approved all associated procedures. Brush biopsy samples were specifically obtained from both scar and normal tracheal epithelium. For histological analyses, five separate patients with iLTS and five patients with iSGS underwent cricotracheal resection as part of their treatment plan. Normal controls for histologic analysis were rapidly processed autopsy (RPA) specimens processed within 24 hours of death.[16] Rapid autopsy tissue samples were excluded from PCR analysis due to concerns of RNA degradations postmortem. Rapid autopsy samples of normal tracheal epithelium were also obtained in accordance with Johns Hopkins University Institutional Review Board (IRB 00250531) and used as non-scar control specimens.

Rt-PCR

Brush biopsies of scar and non-scar epithelium (normal) were obtained from patients with iSGS (n = 4) and iLTS (n = 4) who underwent endoscopic excision and dilation surgery. Brush
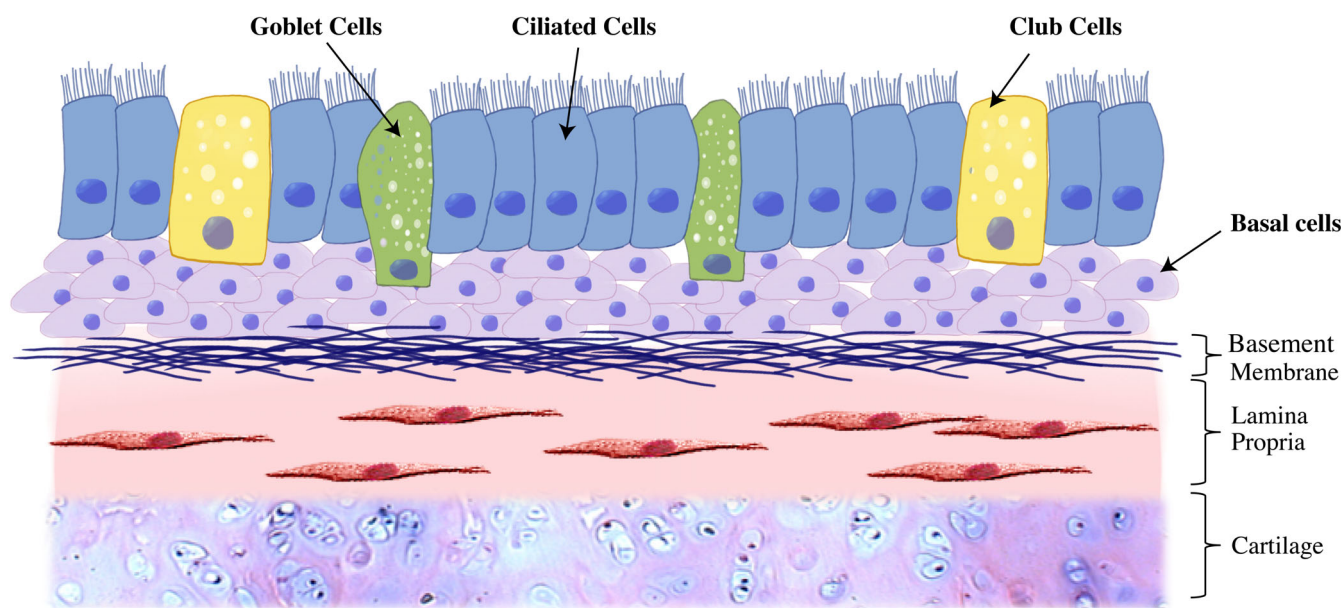

Fig. 1. Epithelium overview.

samples were separate from tissue samples, were mechanically homogenized using metallic microbeads in RLT buffer, and subsequently purified after serial centrifugation and filtration steps using the RNeasy Mini Spin Column as specified in the RNeasy Minikit (Qiagen, Valencia, California), as previously described.[17] RNA was quantified with a NanoDrop 2000 spectrophotometer (Thermo Scientific, Waltham, Massachusetts) converted into cDNA using the iScript cDNA Synthesis Kit (Bio-Rad, Hercules, CA) as per the manufacturer's recommendations. Gene primers (Integrated DNA technologies, Coralville, Iowa) used included Cytokeratin-14 (*CK14*), Cytokeratin-5 (*CK5*), Tumor Protein P63 (*TP63*), Mucin 5AC (*MUC5AC*), Clara cell secreting protein (*CCSP*), Tubulin alpha 1A (*TUBA1A*), and Calmodulin 1 (*CALM1*) (see Supporting Information, Table S1). Gene expression was assessed using quantitative real-time polymerase chain reaction (qPCR) with a StepOnePlus Real-Time PCR system (Life Technologies, Carlsbad, California) and Power SYBR Green Mastermix (Life Technologies). Each reaction well underwent 40 cycles of a denaturation step at 95°C for 15 seconds, followed by annealing and extension at 60°C for 60 seconds. The cycle threshold (CT) for gene product detection was normalized against the reference gene GADPH and then compared with normal controls (ΔΔCT). Gene expression is presented as relative fold change ($2^{-\Delta\Delta\text{CT}}$) and therefore normal controls are normalized to a gene expression of 1. All samples were repeated in triplicate.

Immunohistochemistry and Cell Counting

Tissue section specimens from patients with iSGS (n = 5) and iLTS (n = 5) were compared with non-scar trachea derived from rapid autopsy (RPA) tracheal specimens. These RPA tracheal specimens were selected based on patients with no prior evidence of tracheostomy, prolonged intubation, or history of radiation to the head and neck. Additional demographics are outlined in Table I. Specimens were fixed in 10% formalin for a minimum of 24 hours and subsequently embedded in paraffin. Formalin-fixed, paraffin-embedded (FFPE) tissue blocks were sectioned in 5 μm cuts in axis with tracheal rings (anatomically axial cuts) so as to provide circumferential evaluation of the tracheal epithelium. Prior to staining, slides were deparaffinized and rehydrated using xylene/ethanol. To recover antigenicity, a heat-induced epitope retrieval procedure using a sodium citrate buffer (10 mM Sodium Citrate, 0.05% Tween 20, pH 6.0) and a steamer was performed. To avoid acquiring false-positive staining, slides were washed with 1ml PBS and subsequently incubated for 30 minutes in DMEM with 10% FBS to block unspecific binding sites. Finally, individual slides were incubated using simultaneous immunofluorescence staining and left overnight. Slides were stained for DAPI, Anti-Cytokeratin 14 (CK14, clone LL002, Thermo Scientific, Fremont, CA, USA), and either anti-acetylated α-tubulin (clone 6-11B-1, Santa Cruz Biotechnology, Santa Cruz, CA, USA) or Anti-Muc5ac.a (#BS-7166R, Bioss Inc, USA). For each CK14 stained slide, the number of cells with positive staining for CK14 was measured on 40× (high-powered field) magnification and normalized to total number of cells present in the epithelium at that magnification. Measurements were taken in triplicate at three different high-powered epithelial locations. Due to a range of total cell counts (59-299), these were normalized to the total number of epithelial cells as a percentage and subsequently averaged per sample. Similarly, the number of positive cells staining for TUBA was also measured and normalized to the total number of most apical cells. These were also performed in triplicate, as described above. A total of three specimens of each group was used for this portion of the analysis.

Standard hematoxylin–eosin (H&E) staining of tissue section specimens were utilized for cell counting and epithelial

thickness, given a limited supply. Only areas of intact epithelium were evaluated to avoid capture of slide processing artifacts, and to reduce inherent observer bias between groups. Epithelial thickness was measured from basement membrane to cell surface (excluding cilia). The number of secretory cells (by counting vacuolated cells) within intact epithelium were counted at 40× magnification and normalized to total cell number per slice. Measurements were taken in triplicate at three different high-powered fields and averaged per sample.

Statistical Analysis

Multiple groups were compared using an analysis of variance (ANOVA) with a Bonferroni correction for multiple comparisons. Categorical patient demographic data were compared with a Fisher exact test. Continuous patient demographics were compared with a Mann–Whitney test. Significance criterion for all analyses was set at $P < .05$. Data analysis was performed using Prism software (version 8.4.3, GraphPad Software Inc., CA, USA).

RESULTS

Experimental Cohort

Patient demographics can be seen in Table I. For endoscopic tissue samples, there were no significant differences in age, sex, or Cotton–Meyer grade between iLTS and iSGS. Patients with iLTS were more likely to have a history of tracheostomy ($P = .03$) and a high BMI ($P = .03$). For tissue section derived from patients who underwent cricotracheal resection, there were no differences in age, sex, or BMI. Rapid autopsy samples expectedly had greater Charlson comorbidity index (CCI) scores than the experimental arms ($P = .005$).

Epithelial Thickness is Reduced in iLTS-Scar and iSGS-Scar Compared with Non-Scar Controls

H&E staining of tissue section specimens shows epithelial thickness in iLTS (n = 5) and iSGS (n = 5) compared with control (Rapid autopsy specimens, n = 5) epithelium (Fig. 2A). Quantitative assessment showed a reduction in iLTS-scar epithelium (mean of 71.7 μm, mean difference of 46.97 μm, $P = .0011$, 95% CI: 21.06–72.87) and iSGS-scar epithelium (mean of 70.3 μM, mean difference of 48.37 μm, $P = .0009$, 95% CI: 22.47–74.27) compared with non-scar RPA controls (mean of 118.7 μm) (Fig. 2B).

Gene Expression of Basal Cell Markers Cytokeratin 14 (CK14) and 5 (CK5) are Increased in iSGS-Scar Epithelium

Brush biopsies of iSGS-scar showed a 34-fold (n = 4, $P = .027$) increased expression of *CK14* compared with control epithelium (n = 4) and a 30-fold increase compared with iLTS (n = 4, $P = .049$) (Fig. 3A). *CK5* was also elevated in iSGS-scar brush biopsies compared with non-scar epithelial (7.1×, $P = .034$) and iLTS-scar (5.1×, $P = .033$). *TP63* expression was not different in control

TABLE I.
Patient Demographics.

Enrollment	Brush Biopsy			Tissue Section			
	iLTS (n = 4)	iSGS (n = 4)		iLTS (n = 5)	iSGS (n = 5)	RPA (n = 5)	
Mean age (range)	51 (23–81)	50 (39–60)	$P = .93$	48 (20–79)	51 (31–86)	51 (33–67)	$P = .97$
Sex, female (%)	2 (50%)	4 (100%)	$P = .10$	3 (60%)	5 (100%)	2 (40%)	$P = .12$
BMI (range)	32.2	40.6	**$P = .03$**[*]	26.3	25	20.2	$P = .12$
Cotton–Meyer grade	2.8	1.8	$P = .25$	2.6	2.4	–	$P = .58$
1	1	1		0	0	–	
2	1	3		2	3	–	
3	0	0		3	2	–	
4	2	0		0	0	–	
Tobacco use, n							
Current	0	0		0	0	1	
Former	2	0		2	0	0	
Never	4	4		3	5	4	
History of intubation	4	1		5	1	1	
Tracheostomy	4	0	**$P = .03$**[*]	1	1	0	$P = .58$
Comorbidities							
Asthma	0	0		1	0	0	
COPD	0	0		1	0	0	
T2DM	1	1		1	0	1	
Depression	2	1		1	1	3	
GERD	1	1		0	3	1	
Hemiplegia	1	0		0	0	0	
Hypertension	3	3		0	1	0	
OSA	2	0		0	0	0	
Solid tumor	1	0		0	0	5	
Inflammatory tissue disease	0	0		0	0	0	
Steroids	0	0		0	1	2	
Radiation	0	0		0	0	0	
CCI (range)	4 (2–7)	1.3 (0–2)	$P = 0.058$	1.8 (0–5)	1.8 (0–5)	8.4 (2–13)	**$P = .005$**[*]
Level of stenosis							
Posterior glottis	1	0		0	0	–	
Subglottic	2	4		2	4	–	
Tracheal	4	0		3	2	–	
Glottic	1	0		0	0	–	
Multilevel	3	0		1	1	–	

CCI = Charlson Comorbidity Index; COPD = chronic obstructive pulmonary disease; GERD = gastroesophageal reflux disease; OSA = obstructive sleep apnea; T2DM = diabetes mellitus type 2.
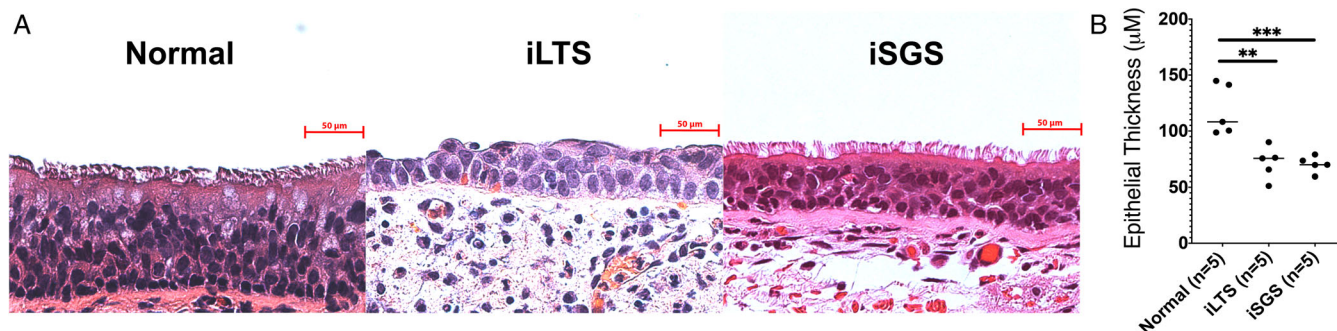[*]Significance statement for bold $P < 0.05$.

Fig. 2. Histological overview and epithelial thickness—(A) Representative H&E stained sections of iLTS-scar, iSGS-scar, and control epithelium. (B) Epithelial thickness (µM) is reduced in both iSGS and iLTS-scar compared with non-scar controls. $*$ = $P < .05$; $**$ = $P < .01$; $***$ = $P < .001$.

Basal Cell Markers

A

CK14, CK5, TP63 scatter plots; Control, iLTS (n=4), iSGS (n=4)

B

CK14 Expression (%Total); Control (n=3), iLTS (n=3), iSGS (n=3)

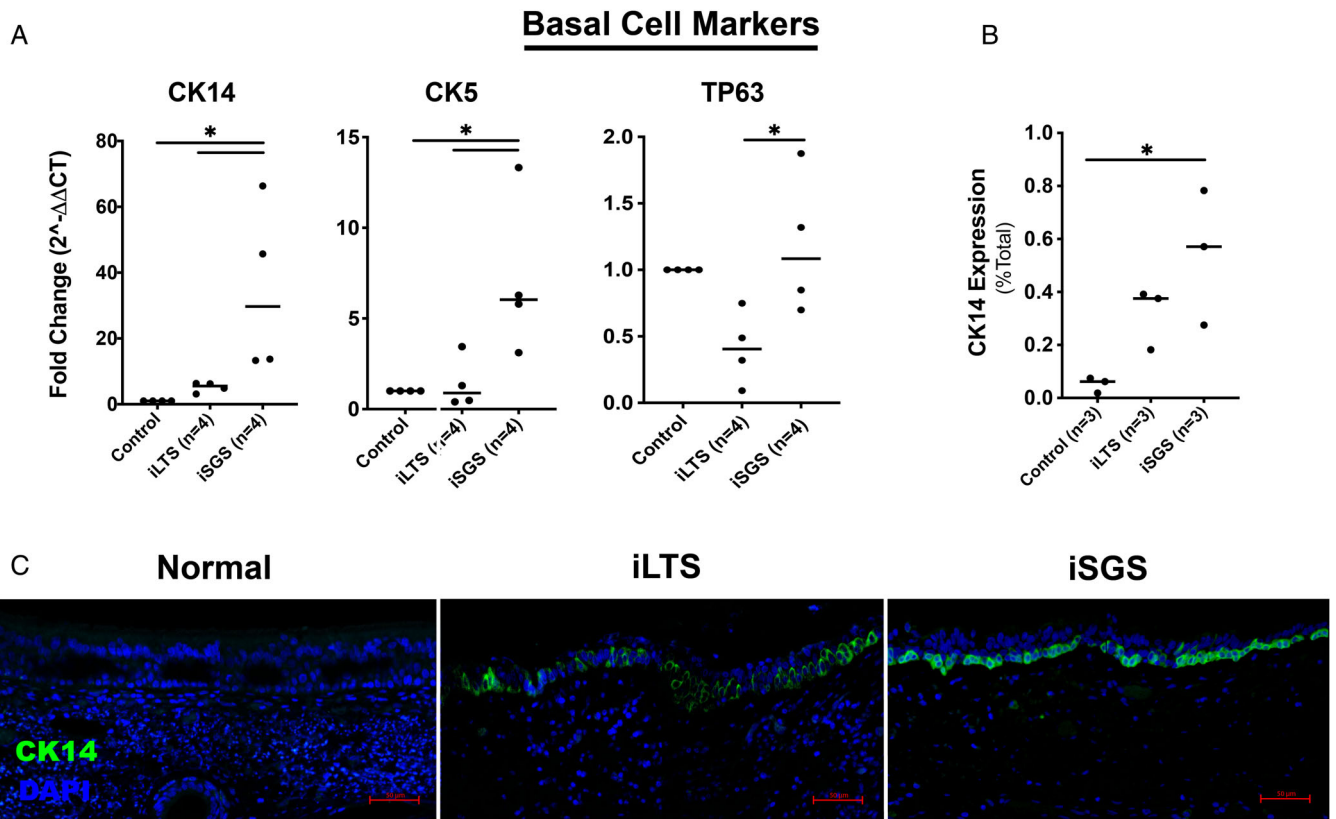C Normal / iLTS / iSGS — CK14 / DAPI immunohistochemical staining

Fig. 3. Increased CK14+ basal cells in iSGS-scar—(A) Gene expression data for pathologic basal cell markers CK14, CK5, TP63 in brush biopsy samples from patients with iLTS and iSGS-scar epithelium compared with normal, non-scar epithelium showing increased CK14 and CK5 expression in iSGS-scar (B) Quantitative analysis of immunohistochemical staining demonstrating increased CK14 expression in iSGS-scar compared with non-scar controls (C) Representative immunohistochemical staining for CK14. * = P < .05; CK14 = cytokeratin 14; CK5 = cytokeratin 5; TP63 = tumor protein 63.

epithelium compared with iSGS or iLTS-scar derived epithelium, yet there was a 2.8-fold reduction in iLTS-scar compared with iSGS-scar epithelium (P = .028, Fig. 3A). Morphologic observations included atypical basal cells in scar samples. In some areas, they were hyperplastic and more densely stacked than normal controls. Quantitative analysis of IHC staining (Fig. 3B,C) revealed a greater percentage of CK14 positive basal cells in iSGS-scar (54% positive per hpf, mean difference 49.1%, n = 3, P = .02, 95% CI: 9.7%–89%) compared with control epithelium (5% positive per hpf, n = 3). There was no difference with iLTS.

Protein Expression of Cilia, But Not Gene Expression, is Diminished in Both iLTS and iSGS Relative to Control Epithelium

There were no significant differences in ciliated cell gene expression (*TUBA1A* or *CALM1*) between LTS and RPA control brush biopsy samples (Fig. 4A). Quantitative immunohistochemical staining (Fig. 4B) for *TUBA1A*, a ciliary marker, showed a significant decrease expression in both iLTS (19.5%, mean difference 61%, n = 3, P = .0125, 95% CI: 17%–105%) and iSGS (24.5%, mean difference 56%, n = 3, P = .0184, 95% CI: 12%–100%) compared with RPA controls (80.5%, n = 3). Immunohistochemistry also demonstrated irregular cilia present in iLTS-scar

epithelium as compared with iSGS-scar or normal epithelium (Fig. 4C). Merged representative immunohistochemical staining demonstrated changes in epithelium morphology in iSGS and iLTS-scar epithelium compared with non-scar epithelium (Fig. 5).

Mucous Producing Goblet Cells are Reduced in Both iLTS and iSGS-Scar Epithelium

iLTS-scar (2.85-fold decrease, n = 4, P = .0035) and iSGS-scar (5.6-fold decrease, n = 4, P = .0007) had a significant reduction in *MUC5AC* gene expression compared with control epithelium (n = 4) (Fig. 6A). Similarly, *CCSP* gene expression was decreased in iLTS (33.4-fold decrease, n = 4, P < .0001) and iSGS-scar (5.3-fold decrease, P < .0002) compared with control epithelium. Further, both iSGS-scar (1.8%, mean difference of 6.1%, n = 5, P < .0001, 95% CI: 4.1%–9.9%) and iLTS-scar epithelium (1.3%, mean difference of 7.5%, n = 5, P < .0001, 95% CI: 4.6%–10.4%) had significantly reduced populations of secretory cells, compared with normal (5.5%, n = 5, P < .0001), control epithelium (Fig. 6B). Representative immunohistochemical staining for MUC5AC demonstrated diminished goblet cell expression in iLTS and iSGS epithelium compared with non-scar epithelium (Fig. 6C).
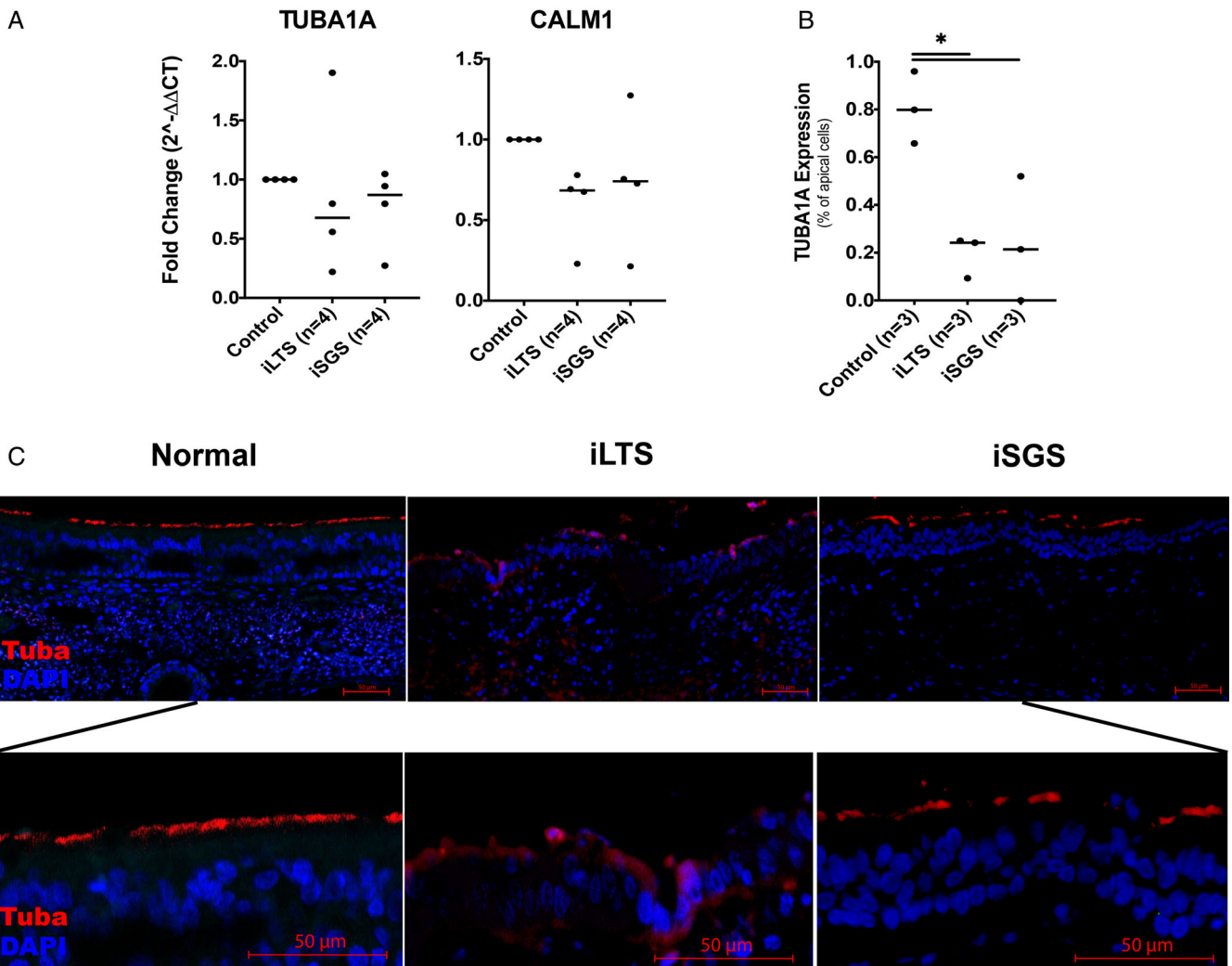
Ciliated Cell Markers

Fig. 4. Diminished ciliary cells in iSGS and iLTS-scar—(A) Gene expression for CALM1 and TUBA1A, two ciliary markers, demonstrated no significant differences between groups. (B) Quantitative analysis of immunohistochemical staining demonstrated decreased TUBA1A expression among apical cells in iLTS and iSGS-scar epithelium compared with non-scar controls. (C) Representative immunohistochemical staining for TUBA1A (TUBA), and DAPI demonstrating abnormal morphology in iLTS and ISGS-scar epithelium compared with non-scar controls; magnified view demonstrating ciliary staining. * = P < .05.
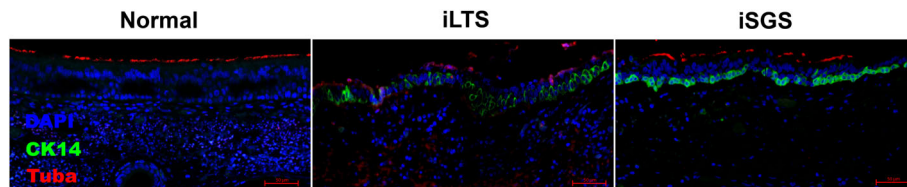

Fig. 5. Changes in epithelial morphology in iLTS and iSGS—Representative immunohistochemical staining for CK14, TUBA1A, and DAPI demonstrating abnormal morphology in iLTS and ISGS-scar epithelium compared with non-scar controls.

DISCUSSION

This is the first study to characterize the epithelium overlying scar in different clinical etiologies of LTS as well as comparing diseased with normal subglottic epithelium. In our data, we observed noticeable differences in multiple epithelial cell types between iSGS-scar, iLTS-scar, and non-scar control epithelium. Compared with non-scar controls, both iSGS-scar and iLTS-scar
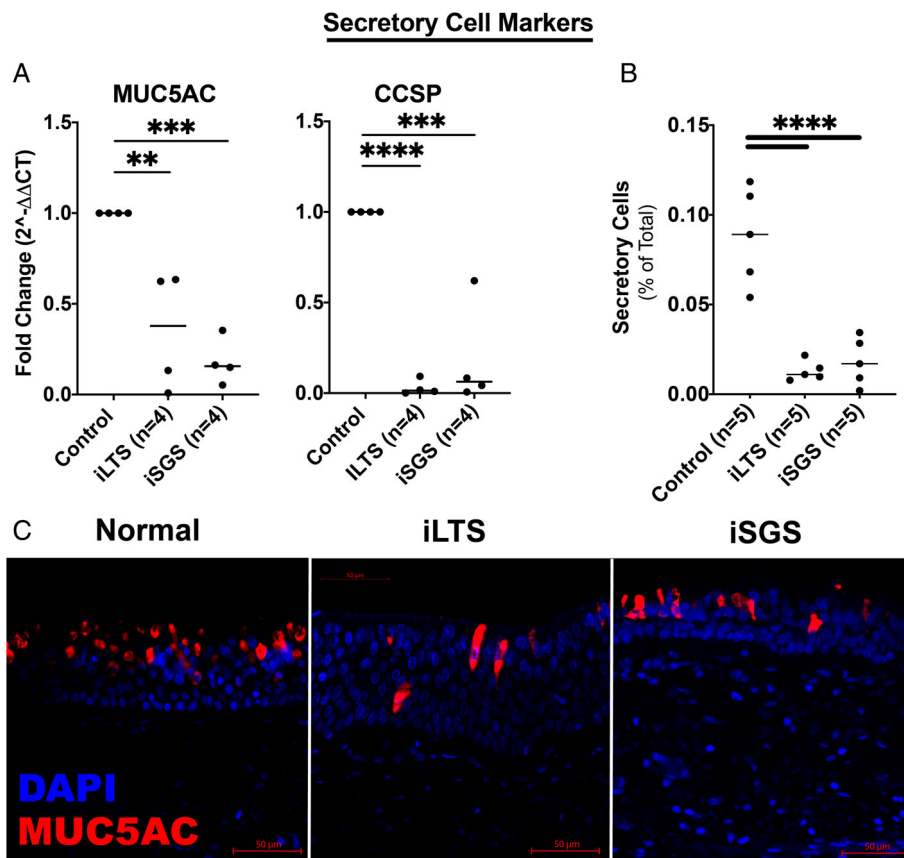
Secretary Cell Markers

Fig. 6. Low secretory cell expression in iSGS and iLTS-scar—(A) MUC5AC and CCSP, two secretory cell markers were significantly reduced in both iSGS and iLTS-scar epithelium compared with non-scar controls. (B) Secretory cells counted on H&E sections were significant reduced in both iSGS and iLTS-scar epithelium. (C) Representative immunohistochemical staining of MUC5AC demonstrated reductions in goblet cells and changes in morphology in iLTS and iSGS-scar epithelium. * = P < .05; ** = P < .01; *** = P < .001; **** = P < .0001.

epithelium had reduced overall epithelial thickness, a reduced number of ciliated cells, and a reduced number of secretory cells, demonstrating abnormal epithelium in both LTS etiologies.

The principal distinction between iSGS and iLTS epithelium was in basal cell morphology. Specifically, we found iSGS-scar epithelium had increased gene expression of *CK5* and *CK14* compared with iLTS epithelium. These pathologic cytokeratin isoforms are seen in other chronic airway diseases[18,19] and demonstrate a diminished capacity for epithelial healing, differentiation, and reductions in tight junction protein expression resulting in abnormal barrier function.[20–24] In IPF specifically, pathologic CK5+CK14+ basal cell subtypes are also associated with regions of active fibrotic disease.[25] This is consistent with our findings within iSGS, which demonstrate pathologic CK5+CK14+ basal epithelium overlying areas of subglottic fibrosis. As the progenitor cell type for club, goblet, and ciliated cells, changes in basal cell morphology also impacts global epithelial function.[26] Interestingly, alterations in epithelial tight junction proteins, which provide a physical barrier between epithelial cells, are present in histological lung samples from patients with IPF and is thought to be associated with fibrosis.[22,27] Similar dysfunctional epithelium may also exist within

iSGS resulting in pathologic healing and subsequent fibrosis.

Comparing and contrasting epithelial morphology between iLTS and iSGS may further our understanding of their respective pathophysiology. In iLTS, the endotracheal tube denudes the epithelium resulting in a limited ability to clear mucus and increasing susceptibility to antigen invasion of the lamina propria.[28] Together this triggers a dysregulated inflammatory cascade, which, in turn, drives fibrosis.[7,29] iSGS, in contrast to iLTS, occurs spontaneously. The presence of atypical epithelial cells in iSGS suggests a common pathogenesis with iLTS, wherein the defects in iSGS epithelium may contribute to the underlying fibrosis. The combination of impaired mucociliary clearance with alterations in epithelial cell barrier function may result in an antigen-induced pro-inflammatory state akin to that found in iLTS. This alteration may contribute to fibrosis within iSGS lamina propria. Future studies should focus on the interaction between the epithelium and the lamina propria to further elucidate this complex relationship and its role in fibrotic development.

While this study is the first to describe epithelial changes in LTS based on clinical phenotype, there are several limitations. As with many translational studies,

our results were limited by a relatively low number of patent samples with heterogeneity typical of human specimens. Due to practical limitations of tissue availability, both non-scar brush biopsies and RPA tissue sections specimen were utilized as controls in our study. We also noted slight differences in protein and gene expression between surface markers from brush biopsy compared with sampled tissue, which may reflect more global morphological differences. Moreover, it is also unclear if patient comorbidities or postmortem changes may have impacted the epithelium. Despite this, we were able to successfully characterize and quantify distinct features of iSGS and iLTS-scar epithelium. Although our study did not find differences in ciliary cell gene expression between iLTS and iSGS, this may be secondary to differences in post-translational modifications that are required for ciliary protein expression on the cell surface.[30] Therefore, using IHC, we were able to directly measure differences in ciliary protein between samples. Future studies to assess ciliary function using ciliary beat frequency or electron microscopy and to assess barrier function using permeability and electrical resistance testing may further characterize the impact of morphological aberrant epithelium in patients with LTS.

CONCLUSIONS

In this study, we found abnormal morphology within multiple epithelial cell types in the two predominant etiologies of LTS. Reductions in epithelial thickness, ciliary cells, and secretory cells were common pathologic features of both iSGS and iLTS, whereas an increased prevalence of CK14+ basal cells was found in iSGS epithelium alone. Impaired mucociliary clearance and diminished barrier function may represent a common pathway in the pro-inflammatory state seen within LTS and contributes to lamina propria fibrosis.

BIBLIOGRAPHY

1. Gelbard A, Francis DO, Sandulache VC, Simmons JC, Donovan DT, Ongkasuwan J. Causes and consequences of adult laryngotracheal stenosis. *Laryngoscope* 2015;125:1137–1143. https://doi.org/10.1002/lary.24956.
2. Gadkaree SK, Pandian V, Best S, et al. Laryngotracheal stenosis: risk factors for tracheostomy dependence and dilation interval. *Otolaryngol Neck Surg* 2017;156:321–328. https://doi.org/10.1177/0194599816675323.
3. Parker NP, Bandyopadhyay D, Misono S, Goding GS. Endoscopic cold incision, balloon dilation, mitomycin C application, and steroid injection for adult laryngotracheal stenosis. *Laryngoscope* 2013;123:220–225. https://doi.org/10.1002/lary.23638.
4. Davis RJ, Lina I, Motz K, et al. Endoscopic resection and mucosal reconstitution with epidermal grafting: a pilot study in idiopathic subglottic stenosis. *Otolaryngol - Head Neck Surg (United States)* 2021;1945998211 028163. (ahead of print). https://doi.org/10.1177/01945998211028163.
5. Daniero JJ, Ekbom DC, Gelbard A, Akst LM, Hillel AT. Inaugural symposium on advanced surgical techniques in adult airway reconstruction: Proceedings of the North American Airway Collaborative (NoAAC). *JAMA Otolaryngol - Head Neck Surg* 2017;143:609–613. https://doi.org/10.1001/jamaoto.2016.4126.
6. Gelbard A, Shyr Y, Berry L, et al. Treatment options in idiopathic subglottic stenosis: protocol for a prospective international multicentre pragmatic trial. *BMJ Open* 2018;8:e022243. https://doi.org/10.1136/bmjopen-2018-022243.
7. Minnigerode B, Richter HG. Pathophysiology of subglottic tracheal stenosis in childhood. *Prog Pediatr Surg* 1987;21:1–7. https://doi.org/10.1007/978-3-642-71665-2_1.
8. Proud D, Leigh R. Epithelial cells and airway diseases. *Immunol Rev* 2011; 242:186–204. https://doi.org/10.1111/j.1600-065X.2011.01033.x.
9. Tharakan A, Dobzanski A, London NR Jr, et al. Characterization of a novel, papain-inducible murine model of eosinophilic rhinosinusitis. *Int Forum Allergy Rhinol* 2018;8:513–521. https://doi.org/10.1002/alr.22072.
10. Hildebrandt F, Benzing T, Katsanis N. Ciliopathies. *N Engl J Med* 2011; 364:1533–1543. https://doi.org/10.1056/nejmra1010172.
11. Haghi M, Hittinger M, Zeng Q, et al. Mono- and cocultures of bronchial and alveolar epithelial cells respond differently to proinflammatory stimuli and their modulation by salbutamol and budesonide. *Mol Pharm* 2015;12: 2625–2632. https://doi.org/10.1021/acs.molpharmaceut.5b00124.
12. Perotin JM, Coraux C, Lagonotte E, et al. Alteration of primary cilia in COPD. *Eur Respir J* 2018;52. https://doi.org/10.1183/13993003.00122-2018.
13. Nishida K, Ghosh B, Chandrala L, et al. Quantifying epithelial plasticity as a platform to reverse epithelial injury. *bioRxiv*. January 2020. doi:https://doi.org/10.1101/2020.01.14.906008
14. Li LF, Kao KC, Liu YY, et al. Nintedanib reduces ventilation-augmented bleomycin-induced epithelial–mesenchymal transition and lung fibrosis through suppression of the Src pathway. *J Cell Mol Med* 2017;21:2937–2949. https://doi.org/10.1111/jcmm.13206.
15. Glass DS, Grossfeld D, Renna HA, et al. Idiopathic pulmonary fibrosis: molecular mechanisms and potential treatment approaches. *Respir Investig* 2020;58:320–335. https://doi.org/10.1016/j.resinv.2020.04.002.
16. Davis RJ, Lina I, Ding D, Engle EL, Taube J, Gelbard A, Hillel AT. Increased expression of PD -1 and PD-L1 in patients with laryngotracheal stenosis. *The Laryngoscope*. 2021;131:967–974. https://doi.org/10.1002/lary.28790
17. Lina I, Tsai H-W, Ding D, Davis R, Motz KM, Hillel AT. Characterization of fibroblasts in iatrogenic laryngotracheal stenosis and Type II diabetes mellitus. *The Laryngoscope*. 2021;131:1570–1577. https://doi.org/10.1002/lary.29026
18. Cole BB, Smith RW, Jenkins KM, Graham BB, Reynolds PR, Reynolds SD. Tracheal basal cells: a facultative progenitor cell pool. *Am J Pathol* 2010; 177:362–376. https://doi.org/10.2353/ajpath.2010.090870.
19. Nakajima M, Kawanami O, Jin E, et al. Immunohistochemical and ultra-structural studies of basal cells, Clara cells and bronchiolar cuboidal cells in normal human airways. *Pathol Int* 1998;48:944–953. https://doi.org/10.1111/J.1440-1827.1998.TB03865.X.
20. Alam H, Sehgal L, Kundu ST, Dalal SN, Vaidya MM. Novel function of keratins 5 and 14 in proliferation and differentiation of stratified epithelial cells. *Mol Biol Cell* 2011;22:4068–4078. https://doi.org/10.1091/mbc.E10-08-0703.
21. Kulkarni T, de Andrade J, Zhou Y, Luckhardt T, Thannickal VJ. Alveolar epithelial disintegrity in pulmonary fibrosis. *Am J Physiol - Lung Cell Mol Physiol* 2016;311:185–191. https://doi.org/10.1152/ajplung.00115.2016.
22. Kojima T, Go M, Takano KI, et al. Regulation of tight junctions in upper airway epithelium. *Biomed Res Int* 2013;2013:947072. https://doi.org/10.1155/2013/947072.
23. Heijink IH, Kuchibhotla VNS, Roffel MP, et al. Epithelial cell dysfunction, a major driver of asthma development. *Allergy Eur J Allergy Clin Immunol* 2020;75:1898–1913. https://doi.org/10.1111/all.14421.
24. Borthwick DW, Shahbazian M, Krantz QT, Dorin JR, Randell SH. Evidence for stem-cell niches in the tracheal epithelium. *Am J Respir Cell Mol Biol* 2012;24:662–670. https://doi.org/10.1165/AJRCMB.24.6.4217.
25. Xu Y, Mizuno T, Sridharan A, et al. Single-cell RNA sequencing identifies diverse roles of epithelial cells in idiopathic pulmonary fibrosis. *JCI Insight* 2016;1:e90558. https://doi.org/10.1172/jci.insight.90558.
26. Smirnova NF, Schamberger AC, Nayakanti S, Hatz R, Behr J, Eickelberg O. Detection and quantification of epithelial progenitor cell populations in human healthy and IPF lungs. *Respir Res* 2016;17. https://doi.org/10.1186/s12931-016-0404-x.
27. Zou J, Li Y, Yu J, et al. Idiopathic pulmonary fibrosis is associated with tight junction protein alterations. *Biochim Biophys Acta Biomembr* 2020; 1862:183205. https://doi.org/10.1016/J.BBAMEM.2020.183205.
28. Alexopoulos C, Jansson B, Lindholm C-E. Mucus transport and surface damage after endotracheal intubation and tracheostomy. an experimental study in pigs. *Acta Anaesthesiol Scand* 1984;28:68–76. https://doi.org/10.1111/j.1399-6576.1984.tb02014.x.
29. Hillel AT, Ding D, Samad I, Murphy MK, Motz K. T-Helper 2 lymphocyte immunophenotype is associated with iatrogenic laryngotracheal stenosis. *Laryngoscope* 2019;129:177–186. https://doi.org/10.1002/lary.27321.
30. Gry M, Rimini R, Strömberg S, et al. Correlations between RNA and protein expression profiles in 23 human cell lines. *BMC Genomics* 2009;10:1, 10.1186/1471-2164-10-365–14.